J|A|C|S
ARTICLES

# Ion Permeability of SAMs on Nanoparticle Surfaces

Timo Laaksonen, Outi Pelliniemi, and Bernadette M. Quinn*

*Contribution from the Laboratory of Physical Chemistry and Electrochemistry, Helsinki
University of Technology, P.O. Box 6100, FIN-02015 HUT, Finland*

Received July 3, 2006; E-mail: bquinn@iki.fi

***Abstract:*** This article reports on the ion permeability of self-assembled monolayers (SAMs) formed on the surface of charged alkanethiol-protected gold nanoparticles, so-called monolayer-protected clusters (MPCs). The capacitance and thus the charging energy required to add/remove an electron from the metal core are extremely sensitive to ions entering the monolayer, and the extent of ion penetration can be tuned by the charge and size of the ions and the permittivity of the solvent. Experimentally, this effect is comparable to ion association with conventional redox molecules, indicating that MPCs despite their large size and the fundamentally differing nature of the electron transfer process can be treated analogously to redox molecules.

## Introduction

During the past decade, controlled modification of the interfacial properties of electrodes using self-assembled monolayers (SAMs) has generated enormous interest.[1] The reactivity, adhesion, wetting, electrical, and structural properties of the electrode surface can be tailored simply by changing the adsorbate molecule used to form the SAM.[1] In particular, SAMs formed due to the adsorption of alkanethiols on planar metal surfaces have been widely used in fundamental studies of long-range electron transfer (ET) reactions.[1a,d,2] Typically, experimental conditions are chosen such that the SAM presents a barrier of controlled thickness to ET between a solution redox species and the underlying electrode; that is, the SAM should be impermeable to both ions in solution and the redox species.[1a,c,2a,b,e,3] Ion permeability of these planar SAMs has been demonstrated to be a property of the adsorbate molecule, the charge of its terminal functional group, and the ordering and packing of the alkyl chains.[1a,c,2b,e,3,4] It is also dependent on applied electrode potential and the solvent used.[2b,3,5] However, much less is known about the barrier properties of comparable SAMs formed on nanoparticle surfaces.[1a,c,6] Due to the high radius of curvature of the nanoparticle core, alkyl chain packing and order decrease with increasing distance from the core.[1a,6,7] Spectroscopic and Taylor dispersion measurements indicate that the SAM terminal groups are considerably less ordered and more fluidlike than their planar counterparts.[7] The effect of this radial ordering on the ion permeability of the SAM has not been considered to date.

Thiol-protected gold nanoparticles, so-called monolayer-protected clusters (MPCs), represent a particular class of SAM-modified nanoparticles.[1a,6] Dispersed MPCs have been considered as both diffusing nanoelectrodes and conventional redox molecules.[6a] Due to a combination of nanometer core size and the sub-attofarad capacitance associated with the protecting monolayer, electron transfer to the metal core is discrete and single electron/hole charging occurs at regularly spaced potential intervals, $\Delta E$.[6a] As the monolayer capacitance determines the charging properties ($C = e/\Delta E$), SAM permeability to ions will influence electron transfer to the metal core. However, unlike long-range ET between macroscopic SAM-modified electrodes and a solution or SAM-attached redox species, the MPC itself is the redox species. Thus, it is the permeability of the MPC SAM to counterions and solvent that determines both the kinetics and thermodynamics of ET reactions with MPC redox species. Ion-gated electron transfer has been reported for planar SAMs where the permeability of the monolayer was modified

---

(1) (a) Love, J. C.; Estroff, L. A.; Kriebel, J. K.; Nuzzo, R. G.; Whitesides, G. M. *Chem. Rev.* **2005**, *105*, 1103. (b) Ulman, A. *Chem. Rev.* **1996**, *96*, 1533. (c) Badia, A.; Lennox, R. B.; Reven, L. *Acc. Chem. Res.* **2000**, *33*, 475. (d) Adams, D. M.; et al. *J. Phys. Chem. B* **2003**, *107*, 6668. (e) Fendler, J. H. *Chem. Mater.* **2001**, *13*, 3196.

(2) (a) Porter, M. D.; Bright, T. B.; Allara, D. L.; Chidsey, C. E. D. *J. Am. Chem. Soc.* **1987**, *109*, 3559. (b) Finklea, H. O. *Electroanal. Chem.* **1996**, *19*, 109. (c) Smalley, J. F.; Sachs, S. B.; Chidsey, C. E. D.; Dudek, S. P.; Sikes, H. D.; Creager, S. E.; Yu, C. J.; Feldberg, S. W.; Newton, M. D. *J. Am. Chem. Soc.* **2004**, *126*, 14620. (d) Chidsey, C. E. D. *Science* **1991**, *251*, 919. (e) Liu, B.; Bard, A. J.; Mirkin, M. V.; Creager, S. E. *J. Am. Chem. Soc.* **2004**, *126*, 1485. (f) Smalley, J. F.; Finklea, H. O.; Chidsey, C. E. D.; Linford, M. R.; Creager, S. E.; Ferraris, J. P.; Chalfant, K.; Zawodzinsk, T.; Feldberg, S. W.; Newton, M. D. *J. Am. Chem. Soc.* **2003**, *125*, 2004. (g) Wold, D. J.; Haag, R.; Rampi, M. A.; Frisbie, C. D. *J. Phys. Chem. B* **2002**, *106*, 2813. (h) Finklea, H. O.; Yoon, K.; Chamberlain, E.; Allen, J.; Haddox, R. *J. Phys. Chem. B* **2001**, *105*, 3088. (i) Creager, S.; Yu, C. J.; Bamdad, C.; O'Connor, S.; MacLean, T.; Lam, E.; Chong, Y.; Olsen, G. T.; Luo, J.; Gozin, M.; Kayyem, J. F. *J. Am. Chem. Soc.* **1999**, *121*, 1059.

(3) (a) Boubour, E.; Lennox, R. B. *Langmuir* **2000**, *16*, 4222. (b) Boubour, E.; Lennox, R. B. *Langmuir* **2000**, *16*, 7464. (c) Boubour, E.; Lennox, R. B. *J. Phys. Chem. B* **2000**, *104*, 9004. (d) Protsailo, L. V.; Fawcett, W. R. *Langmuir* **2002**, *18*, 8933.

(4) (a) Valincius, G.; Niaura, G.; Kazakevičienė, B.; Talaikytė, Z.; Kažemėkaitė, M.; Butkus, E.; Razumas, V. *Langmuir* **2004**, *20*, 6631. (b) Cannes, C.; Kanoufi, F.; Bard, A. J. *Langmuir* **2002**, *18*, 8134. (c) Calvente, J. J.; Lopez-Perez, G.; Ramirez, P.; Fernandez, H.; Zon, M. A.; Mulder, W. H.; Andreu, R. *J. Am. Chem. Soc.* **2005**, *127*, 6476. (d) Campbell, D. J.; Herr, B. R.; Hulteen, J. C.; Van Duyne, R. P.; Mirkin, C. A. *J. Am. Chem. Soc.* **1996**, *118*, 10211. (e) Sumner, J. J.; Creager, S. E. *J. Phys. Chem. B* **2001**, *105*, 8739. (f) Slowinski, K.; Slowinska, K. U.; Majda, M. *J. Phys. Chem. B* **1999**, *103*, 8544.

(5) Ravenscroft, M. S.; Finklea, H. *J. Phys. Chem. B* **1994**, *98*, 3843.

(6) (a) Templeton, A. C.; Wuelfing, W. P.; Murray, R. W. *Acc. Chem. Res.* **2000**, *33*, 27. (b) Daniel, M.-C.; Astruc, D. *Chem. Rev.* **2004**, *104*, 293. (c) Shenhar, R.; Rotello, V. M. *Acc. Chem. Res.* **2003**, *36*, 549.

(7) (a) Wuelfing, W. P.; Templeton, A. C.; Hicks, J. F.; Murray, R. W. *Anal. Chem.* **1999**, *71*, 4069. (b) Hostetler, M. J.; Stokes, J. J.; Murray, R. W. *Langmuir* **1996**, *12*, 3604.

10.1021/ja064701t CCC: $33.50 © 2006 American Chemical Society

by controlling the charge-compensating counterion size and/or monolayer structure, which in turn controlled the energetics of the ET reaction under study.[4d] For MPCs, it is likely that the discrete charging of the core can radically affect the barrier properties of the SAM and that the monolayer permeability can be similarly gated through the size of the counterion in solution and the dielectric properties of the solvent. Thus, particles of the same composition are anticipated to show markedly different charging behavior simply by altering the counterions in solution.

Previously, a simple concentric sphere capacitor model based on the electrostatic charging of a metallic core has proved successful in describing MPC capacitance for the most widely studied MPC, $Au_{147}$ for low core charge, $z$, where charging peaks occur at regular potential intervals.[6a,8] In some instances, irregularities in $\Delta E$ have been noted at high core charge, $|z| > 4$.[8,9] Also typically for the same particles, $\Delta E$ is dependent on the charge sign of the particles, i.e., whether the particles are undergoing oxidation or reduction.[10] The difference between reports is likely to be due to medium effects: the solvent and base electrolyte used in the electrochemical measurements and thus the barrier properties of the monolayer. Here we demonstrate that charged MPCs can associate with base electrolyte ions, and this interaction induces changes in $\Delta E$ analogous to ion-pairing phenomena noted for conventional redox species, e.g., bis(fulvalene)dinickel.[11] However unlike with conventional molecules, association here is a measure of the ion permeability of the protecting monolayer. In this study, MPCs from the same synthesis batch were dispersed in solvents with differing dielectric constants, 1,2-dichloroethane (DCE) and chlorobenzene (CB) ($\epsilon = 10.24$ and 5.6, respectively),[12] and MPC charging was investigated in the presence of a series of base electrolytes comprised of ions with contrasting sizes, hydrophilicities, and charge distributions. The dispersing medium profoundly influences the monolayer capacitance, and this effect is more marked as the core charge is increased. We show that the choice of base electrolyte determines the amount of energy required to achieve a given MPC charge and demonstrate that this can be used as a simple measure of the ion permeability of SAMs formed on nanoparticle surfaces.

## Experimental Section

**Chemicals.** The solvents considered, 1,2-dichloroethane (DCE) and chlorobenzene (CB), were obtained from Sigma (spectroscopic grade) and Fluka (p.a.), respectively, and used as received. All other chemicals were of the highest commercially available purity. The base electrolytes used, tetraphenylarsonium pentafluorophenyl borate ($TPAsTPBF_{20}$) and tetraethylammonium pentafluorophenyl borate ($TEATPBF_{20}$) salts, were prepared by metathesis of the corresponding chloride, TPAsCl (Fluka) and TEACl with $KTPBF_{20}$ (Boulder Scientific) in a 2:1 mixture of methanol and water. The resulting precipitates were filtered, washed, and recrystallized from acetone. Tetrabutylammonium hexafluorophosphate ($TBAPF_6$) was prepared similarly by metathesis of tetrabutylammonium chloride and lithium hexafluorophosphate.

Hexanethiolate MPCs (C6 MPCs) were synthesized according to a literature procedure known to yield particles of small core diameter.[13] The synthesis yields particles with a dominant population of monodisperse cores of average radius of 0.81 nm as determined from electrochemical measurements,[10] where the appearance of regularly spaced charging peaks in the presence of the base electrolyte $TPAsTPF_{20}$ indicates that the particles are highly monodisperse. The average core size was estimated using the simple concentric sphere capacitor model to describe the MPC capacitance, and the particles were assigned $Au_{147}$ based on previous reports.[6a,8,9] Particles from the same synthesis batch were used throughout.

**Electrochemical Measurements.** Cyclic voltammetry (CV) and square wave voltammetry (SQV) measurements were performed using a CHI-900 potentiostat (CH-Instruments, TX). A two-electrode arrangement was used where a silver wire was used as both quasi-reference electrode (QRE) and counter electrode. The working electrode used throughout was a Pt microelectrode ($d = 25\ \mu$m). Measurements were performed in the absence of MPCs for each solvent/base electrolyte system to ensure that the potential window was featureless. Solutions were purged with $N_2$ to remove $O_2$ from solution and extend the potential window available at negative electrode potentials. Experimental results could be interpreted solely in terms of the base electrolyte used, as particles from the same synthesis were used for all measurements. Particles were purified using multiple precipitation/washing/dispersion cycles. The particles were precipitated from solution by the addition of a nonsolvent such as acetonitrile, and the precipitate was rinsed well and then redispersed in DCE. A minimum of three separate measurements per solvent/base electrolyte were performed, and the observed charging behavior was repeatable (±10 mV). It was completely independent of the sequence of solvents/base electrolytes used.

## Results and Discussion

The redox properties of the MPCs were followed voltammetrically at a Pt microelectrode, where the particles were dispersed in differing solvent/base electrolyte systems. The voltage separation $\Delta E$ between charging events was measured with square wave voltammetry (SWV), and typical plots obtained are shown in Figure 1. The current peaks correspond to the half-wave potentials for the $z/(z \pm 1)$ charge states and the current minima for the $z$ states.[6a] The maximum peak separation is at the MPC potential of zero charge and was assigned as that between the $-1/0$ and $0/+1$ charges as previously reported.[9a,10] Representative plots of peak separation versus charge state are given in Figure 2. As is obvious from the figures, the charging peaks are both most clearly defined and regularly spaced for the DCE/$TPAsTPBF_{20}$ case, where up to 14 distinctive charging peaks can be seen. Simply changing the base electrolyte to include ions such as $PF_6^-$ or $TEA^+$ has a profound effect on the peak separation. As can be seen in Figures 1a and 2a, $\Delta E$ in the presence of $TBAPF_6$ for $z > 0$ decreases with increasing core charge from 280 mV to ca. 150 mV, and the peaks "wash out" completely at higher charge states. Changing the solvent from DCE to CB ($TBAPF_6$ case, $TEATPBF_{20}$ is not sufficiently soluble in CB) induced a more pronounced decrease already at lower core charge. Again the peak resolution washes out at higher core charges. The peak separation for $-1$ and $-2$ charge states was irregular for all

---

[8] Hicks, J. F.; Miles, D. T.; Murray, R. W. *J. Am. Chem. Soc.* **2002**, *124*, 13322.

[9] (a) Guo, R.; Georganopoulou, D.; Feldberg, S. W.; Donkers, R.; Murray, R. W. *Anal. Chem.* **2005**, *77*, 2662. (b) Miles, D. T.; Murray, R. W. *Anal. Chem.* **2003**, *75*, 1251.

[10] Quinn, B. M.; Liljeroth, P.; Ruiz, V.; Laaksonen, T.; Kontturi, K. *J. Am. Chem. Soc.* **2003**, *125*, 6644.

[11] (a) Barriere, F.; Geiger, W. E. *J. Am. Chem. Soc.* **2006**, *128*, 3980. (b) Barriere, F.; Camire, N.; Geiger, W. E.; Mueller-Westerhoff, U. T.; Sanders, R. *J. Am. Chem. Soc.* **2002**, *124*, 7262.

[12] (a) *Liquid−liquid interfaces, Theory & Methods*; Volkov, A. G., Deamer, D. W., Eds.; CRC Press: Boca Raton, 1996. (b) Nie, B.; Stutzman, J.; Xie, A. *Biophys. J.* **2005**, *88*, 2833.

[13] (a) Chen, S.; Ingrma, R. S.; Hostetler, M. J.; Pietron, J. J.; Murray, R. W.; Schaaff, T. G.; Khoury, J. T.; Alvarez, M. M.; Whetten, R. L. *Science* **1998**, *280*, 2098. (b) Brust, M.; Walker, M.; Bethell, D.; Schiffrin, D. J.; Whyman, R. *Chem. Commun.* **1994**, 801.

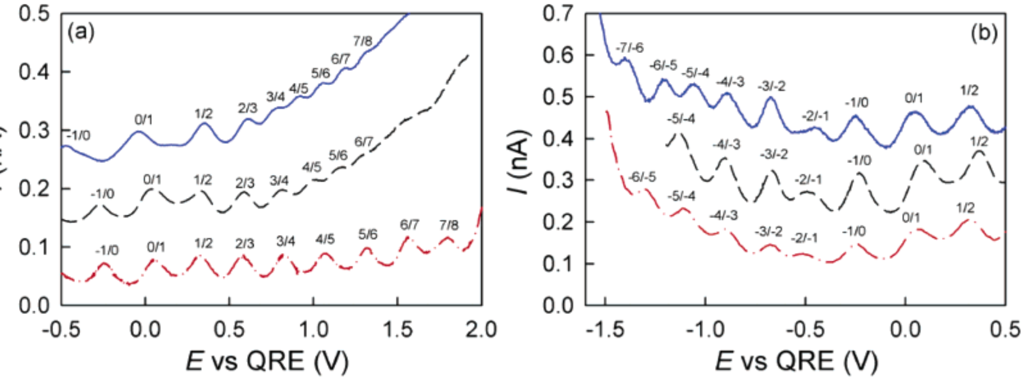

***Figure 1.*** Measured SWV plots showing discrete charging of MPCs in the presence of different electrolytes: (a) focusing on the positive potential region, $TBAPF_6$ in CB (solid line), $TBAPF_6$ in DCE (dashed), and $TPAsTPBF_{20}$ in DCE (dash−dot); (b) focusing on the negative potential region in the presence of $TEATPBF_{20}$ (solid line), $TBAPF_6$ (dashed), and $TPAsTPBF_{20}$ (dash−dot). The base electrolyte concentration was 10 mM in all cases. (The plots are offset on the current axis for clarity.)

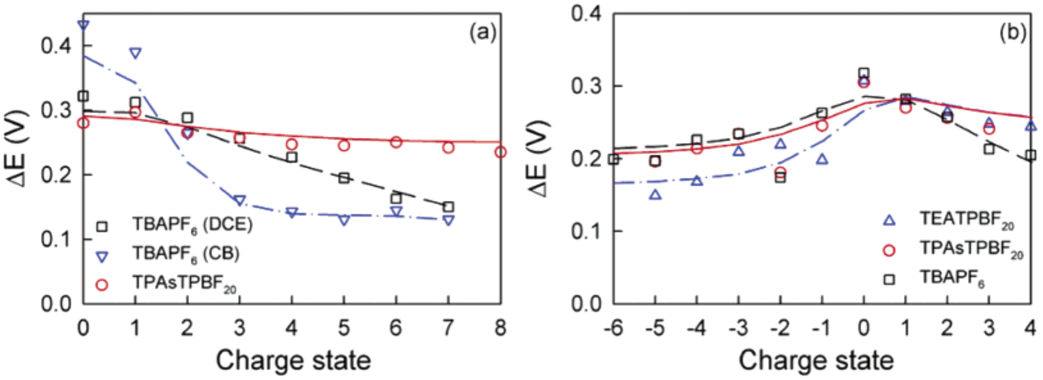

***Figure 2.*** (a) Measured peak separations (symbols) and the corresponding best fits obtained using the ion penetration model (lines) vs particle charge state for MPCs dispersed in differing solvent/base electrolytes. (a) $z > 0$, circles $TPAsTPBF_{20}$ in DCE, squares $TBAPF_6$ in DCE, triangles $TBAPF_6$ in CB. The fitting parameter $\alpha$ was gradually decreased from 1 to 0.6 for $TBAPF_6$ in DCE (dashed line). For $TBAPF_6$ in CB (dash−dot), $\alpha$ varied from 0.95 for $z = +1$ to 0.44 for $z = +7$, and for $TPAsTPBF_{20}$ in DCE (solid line) no ion penetration was assumed ($\alpha \geq 1$). (b) Squares $TBAPF_6$, triangles $TEATPBF_{20}$, circles $TPAsTPBF_{20}$ all in DCE. The fitting parameter $\alpha$ was gradually decreased from 1 to 0.6 for $TBAPF_6$ in DCE (dashed line) for $z > 0$ and was equal to 0.74 for $z < 0$. For $TEATPBF_{20}$ in DCE (dash−dot) $\alpha = 0.49$ for $z < 0$, and with $TPAsTPBF_{20}$ in DCE (solid line) $\alpha = 0.70$ for $z < 0$. $TPBF_{20}^-$ was assumed not to penetrate the ligand shell. $\Delta E$ for −1 and −2 are irregular due to film formation on the electrode surface.

base electrolytes due to precipitation of the MPCs on the electrode surface, as previously reported.[10] In Figure 2b, it is clear that, for the same base electrolyte anion $TPBF_{20}^-$, changing the cation from $TPAs^+$ to $TEA^+$ markedly decreased $\Delta E$ for $z < -2$, while it remained unchanged for $z > 0$. $TBA^+$ gave a comparable response to $TPAs^+$ for $z < 0$. It should be reiterated that these effects are not artifacts; the data were highly reproducible in that particles could be repeatedly precipitated from solution, washed, and redispersed in another solvent/base electrolyte and consistent data were obtained in each solvent/base electrolyte.

For $z$ close to zero, the peak separation is in line with theoretical predictions when the diffuse layer contribution to the overall MPC capacitance is taken into account.[9a,10] As can be seen in Figure 2, the $\Delta E$ at zero core charge is greater in CB than in DCE for the same base electrolyte, $TBAPF_6$, as expected on the basis of the lower dielectric constant of the former (5.6 versus 10.24).[12] This corresponds to the capacitance minimum for particle double-layer charging, and the value is affected by the dielectric constant of the solvent and electrolyte concentration.[14] However, the large systematic decrease in $\Delta E$ noted here (>100 mV) for higher absolute charges cannot be rationalized from the simple concentric sphere capacitor model nor by taking the contribution of the electrolyte ion diffuse layer into account.[6a,9a,10] The effect of the base electrolyte on peak spacing is comparable to recent reports by Geiger and co-workers for multivalent redox molecules, where the nature of the base ions and the dielectric constant of the solvent strongly influenced the voltage separation between successive electron transfers.[11] It was reported that large, weakly coordinating ions such as $TPBF_{20}^-$ maximized the peak separation, as they ion-paired less significantly with the redox species in comparison to small anions such as $PF_6^-$.[11] However, MPCs are not molecules, and ion-pairing here cannot be described in the conventional sense in terms of the distance of closest approach between ions. As ET to the core depends on the capacitance of the MPC, association in this case reflects the interaction of the base electrolyte ions with the protecting monolayer.

We initially considered association in terms of the effect a layer of specifically adsorbed ions at the periphery of the protecting monolayer would have on the MPC capacitance for the case where the ions do not penetrate the monolayer. A Gouy−Chapman−Stern type model adapted from Valleau and Torrie[15] was used to estimate the MPC capacitance. The solution of the Poisson−Boltzmann equation for the double layer around the particle with appropriate boundary conditions is given in the Supporting Information. In this model, the finite size of the

---

(14) Bard, A. J.; Faulkner, L. R. *Electrochemical Methods, Fundamentals and Applications*, 2nd ed.; John Wiley & Sons Inc.: New York, 2001.

(15) Valleau, J. P.; Torrie, G. M. *J. Chem. Phys.* **1982**, *76*, 4623.

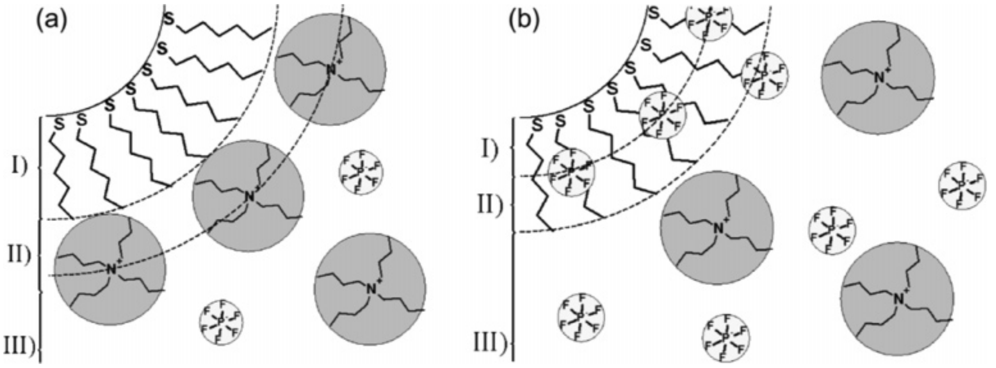

*Figure 3.* (a) Schematic illustration of the ion distribution around a negatively charged MPC ($z < 0$) with counterion adsorption at the monolayer periphery. Area I denotes the extent of the monolayer, area II the distance of closest approach for the counterion, and area III the extent of the diffuse layer. (b) Schematic of a positively charged MPC with counterion penetration to the monolayer. Area I denotes the extent of the ion-free monolayer, area II the extent of counterion penetration in the monolayer, and area III the extent of the diffuse layer.

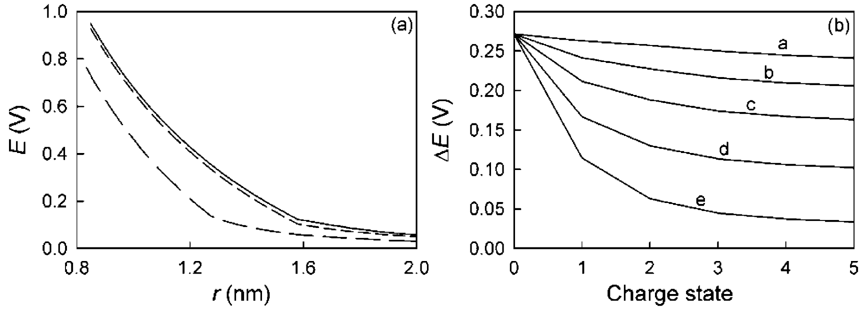

*Figure 4.* (a) Potential distribution around a charged sphere calculated with the standard model[10] (dashed line), with an adsorbed layer (solid line), and with the ion penetration model (long dash). Parameters used in calculations were as follows: $\mathrm{TBAPF_6}$ in DCE, $z = 4$, $r_c = 0.81$ nm, $l = 0.77$ nm, and $\alpha = 0.6$ (solid line). (b) Dependence of peak separation on MPC charge state varying $\alpha$, the parameter describing the extent of ion penetration in the monolayer from 1 (no ion penetration) to 0.05 (significant ion penetration). $\Delta E$ values were estimated using the parameters given above for the following values of $\alpha$; 1.0 (a), 0.75 (b), 0.50 (c), 0.25 (d), and 0.05 (e).

counterions is taken into account by assuming that there is a layer of zero charge density, $\rho$, due to the distance of closest approach next to the particle surface, as shown schematically in Figure 3a. Thus $\rho = 0$ in areas I (extent of the monolayer) and II (extent determined by the radius of the counterion). Area III is the standard electric double-layer region. The potential distributions around a charged MPC obtained using the simple double layer[10] and the adsorbed ion models are compared in Figure 4a. As can be seen from this figure, the difference between models is insignificant. Peak separations calculated as the difference in core potentials between adjacent charge states using this adsorbed ion model do not reproduce the experimental $\Delta E$ values given in Figure 2. In addition, the model predicts a decrease in capacitance (i.e., an increase in $\Delta E$), which is the opposite trend of what was experimentally observed. Thus, adsorption alone is not sufficient to describe ion−MPC interaction.

Next, we considered the situation where ions can enter the monolayer. This is illustrated in Figure 3b. Counterions are assumed to be able to permeate the monolayer up to a fixed distance from the core surface. Outside this region, ions are freely distributed as they would be in a normal double layer. Area I is now the ion-free monolayer, while areas II and III denote the extent of counterion penetration in the monolayer and the extent of the double layer, respectively. Full details of the calculation are presented in the Supporting Information. Briefly, analytical equations by Ohshima[16] were used to calculate potential distributions in areas II and III, and the continuity of potential and surface charge densities at each interface was enforced.

The model parameters are the monolayer dielectric constant and the distance of closest approach of the counterions to the particle core. The dielectric constant of the ion-free monolayer, $\epsilon_l$, is taken as 3.6, as in previous studies.[10] This value was obtained by fitting the experimental data obtained in the presence of the nonpenetrating ion, $\mathrm{TPBF_{20}}^-$, to the spherical double-layer model.[10] The dielectric constant in area II is taken to be the average of the monolayer and the solvent dielectric constants, and the extent of ion penetration, $\alpha$, is defined as

$$\alpha = \frac{a_1 - r_c}{l} \tag{1}$$

where $r_c$ is the radius of the particle core, $l$ the thickness of the ligand shell, and $a_1$ the fitted location of the area I/II boundary as measured from the center of the particle. $\alpha$ has values between 0 and 1, zero indicating complete ion penetration through the monolayer, while unity reflects a completely impermeable monolayer. The effect of ion penetration on the estimated MPC potential distribution is shown in Figure 4a, where it is compared with the double-layer model[10] and the simple adsorption model. As can be seen, the potential drop is more confined in the monolayer upon ion permeation, which affects the core potential of the MPC. This influences $\Delta E$, as it is simply the difference in core potentials for two adjacent charge states. The influence of $\alpha$ on predicted $\Delta E$ values can be clearly seen in Figure 4b. $\Delta E$ drops off precipitously as $\alpha$ is

---

(16) Ohshima, H.; Furusawa, K. *Electrical Phenomena at Interfaces: Fundamentals, Measurements and Applications*; Markcel Dekker: New York, 1998.

decreased from 1 to 0.05. This decrease in $\Delta E$ with increasing particle charge $z$ is of a comparable magnitude to that experimentally observed (Figure 2) depending on the choice of $\alpha$.

We next compared the experimental data to simulation, and the corresponding best fits are also shown in Figure 2. In the calculations, $\alpha$ was varied to get a good fit between the theoretical and experimental curves. The constants used were $\epsilon_l = 3.6$, $r_c = 0.81$ nm, and $l = 0.77$ nm. Base electrolyte ion-paring in the low dielectric solvents was taken into account using the well-known association theory by Bjerrum[17] to estimate the free ion concentrations (see Supporting Information for details). All the cations considered were found to penetrate the monolayer for $z < 0$ with $TEA^+$ penetrating most ($\alpha = 0.49$) and $TBA^+$ and $TPAs^+$ being comparable ($\alpha \approx 0.74$). For $z > 0$, the best fit for $PF_6^-$ in DCE was obtained by allowing $\alpha$ to gradually change from 1.0 to 0.6 with increasing charge. With the same ion in CB, the best fit was obtained by keeping $\alpha$ close to 0.9 in the first two charge states and then letting it quickly drop down to 0.44. With the base electrolyte composed of the largest anion, $TPBF_{20}^-$, the best fit obtained was for $\alpha \geq 1$, i.e., no ion penetration to the monolayer. As expected, $TEATPBF_{20}$ and $TPAsTPBF_{20}$ gave comparable $\Delta E$ within experimental error for $z > 0$ as the counterion is common to both, while for $z < 0$, $\Delta E$ was dependent on the extent of cation penetration in the monolayer.

The extent of ion penetration is surprisingly large. For example, the $\alpha$ value of 0.49 for $TEA^+$ means that the ion is located only 3.8 Å from the surface of the nanoparticle metal core, a very short distance compared to its hard sphere radius of 3.4 Å.[12a] A summary of these values for each ion is given in Table 1. It is evident there is a direct correlation between ion size and the absolute distance ($a_1 - r_c$) the ion can approach the core, smaller ions being able to penetrate the monolayer most. Thus it is clear that small counterions can move far more freely inside the alkanethiol monolayer than previously realized. This size dependence of ion penetration into the SAM on the MPC surface is a direct consequence of the radial ordering of the monolayer; that is, alkyl chain order decreases with increasing distance from the core.

To account for the values of $\alpha$ obtained in different solvents, we have to consider the energetics of ion solvation in the monolayer relative to the bulk solvent. The simple Born model can be used to give an estimate for the difference in the Gibbs energy of solvation $\Delta G$ for small ions in solvents of differing $\epsilon$.[12a]

$$\Delta_{\mathrm{m}}^{\mathrm{s}} G = -\frac{N_{\mathrm{A}} z^2 e^2}{8\pi\epsilon_0 r_{\mathrm{ion}}}\left(\frac{1}{\epsilon_{\mathrm{s}}} - \frac{1}{\epsilon_{\mathrm{m}}}\right) \tag{2}$$

where subscripts m and s refer to the monolayer and solvent, respectively.

Depending on the core charge, the electrostatic potential difference between bulk solution and particle core can be hundreds of millivolts, which may be sufficient to overcome the difference in the Gibbs energy of solvation for small ions.[12a] If we compare $\Delta G$ values from eq 2 obtained for $PF_6^-$ between DCE/monolayer and CB/monolayer, 930 and 510 meV, respectively, significantly less energy is required to transfer the ion from bulk solvent to the monolayer when the solvent and monolayer dielectric permittivities are comparable. Calculations done show that the potentials at the nanoparticle core are sufficient to overcome the energy difference: 1020 mV with $z = 4$ in DCE and 620 mV with $z = 2$ in CB. This is consistent with experimental observation, i.e., increased ion penetration in CB compared to DCE and thus lowered $\Delta E$ (Figure 2a). The gradual decrease in $\Delta E$ with increasing $z$ noted in DCE corresponds to electrostatic potential driven transfer of $PF_6^-$ from DCE to the monolayer. In contrast, $\Delta E$ for $PF_6^-$ in CB reaches a constant value for $z > +2$, indicating that solvents having a dielectric constant close to that of the monolayer facilitate ion penetration into the monolayer.

**Table 1.** Summary of $\alpha$ Obtained from Fitting $a_1 - r_c$ Values and Ionic Radii[12a,18]

| | $a$ | $a_1 - r_c$/Å | $r_{ion}$/Å |
|---|---|---|---|
| $PF_6^-$ (CB) | 0.35 | 2.7 | 1.8[18] |
| $PF_6^-$ (DCE) | 1−0.6 | 7.7−4.6 | 1.8[18] |
| $TEA^+$ (DCE) | 0.49 | 3.8 | 3.4[12a] |
| $TBA^+$ (DCE) | 0.74 | 5.7 | 4.1[12a] |
| $TPAs^+$ (DCE) | 0.70 | 5.4 | 4.3[12a] |
| $TPBF_{20}^-$ (DCE)[a] | 1 | 7.7 | 4.2[12a] |

[a] The radii for tetraphenylborate and $TPBF_{20}^-$ are assumed to be comparable; thus, the literature value of the former was used.

From Figure 2, it is clear that the MPC charge and the counterion in solution determine $\Delta E$. Thus, for $z > 0$, the base electrolyte anion determines $\Delta E$ but has no effect for $z < 0$ and vice versa for cations. Comparable decreases in $\Delta E$ with increasing core charge in the presence of the base electrolyte anions $PF_6^-$ and perchlorate are apparent in experimental data reported previously in the literature but have not been addressed to date.[8,9] In a recent report by the Murray group, the influence of supporting electrolyte and solvent on MPC capacitance was investigated for charge states close to the MPC potential of zero charge.[9a] The observed decrease in MPC capacitance with increasing alkylammonium chain length (C4 to C8) was attributed to increased solvation/penetration of the monolayer due to interdigitation of the longer hydrophobic chains with the alkanethiol monolayer.[9a] On the basis of our results, these findings can now be rationalized by decreased ion penetration with increasing ion size, which results in decreased capacitance. Also from our data, very hydrophobic ions such as $TPBF_{20}^-$ [12a] do not influence the MPC capacitance, indicating hydrophobicity is not the critical parameter influencing the capacitance. Although $TPBF_{20}^-$ and $TPAs^+$ are of comparable size, the former does not penetrate the monolayer. This suggests that the ion properties also play a role in monolayer permeability.

Charge delocalization has a significant effect on the strength of ion−ion interactions.[19] For conventional redox molecules, systematic variation of solvent and supporting electrolyte showed that $\Delta E$ values for sequential one-electron redox processes in nonaqueous solutions were strongly medium dependent.[11] The experimental trends noted are comparable to those reported here. Large, weakly coordinating ions such as $TPBF_{20}^-$ in low-permittivity solvents maximize $\Delta E$.[11a] However, the nature of the interaction differs in that, with conventional redox species, it is the extent of ion-pairing between the charged redox species and the base electrolyte ions that determines $\Delta E$.

---

(17) Bockris, J. O. M.; Reddy, A. K. N. *Comprehensive Treatise of Electrochemistry. Volume 1; The Double Layer*, 2nd ed.; Plenum Press: New York, 1998.

(18) Thompson, M. A. ArgusLab 4.0.1; Planaria Software LLC: Seattle, WA, http://www.arguslab.com.

(19) Krossing, I.; Raabe, I. *Angew. Chem., Int. Ed.* **2004**, *43*, 2066.

In contrast with MPCs, $\Delta E$ is determined by the ability of base electrolyte ions to enter the monolayer.

## Conclusions

We have demonstrated that the discrete charging of the MPC core directly affects the permeability of the protecting monolayer. As the monolayer permeability determines the MPC capacitance, this is turn determines redox properties. $\Delta E$ is comparable for all base electrolytes in the same solvent for $z = 0$; that is, ions do not enter the monolayer without an electrostatic driving force between the core and bulk solution. Order and chain packing decrease with increasing distance from the core, making solvent and ion penetration to the monolayer more likely than at their planar counterparts. The extent of SAM ion permeability is dependent on the core charge, the dispersing solvent, and the base electrolyte ions in solution. Thus, the redox properties of dispersed MPCs offer a very simple means to probe the ion permeability of SAMs formed on nanoparticle surfaces.

**Acknowledgment.** Financial support from the Academy of Finland is acknowledged.

**Supporting Information Available:** Additional details on the solution of the Poisson−Boltzmann equation for both the adsorption and ion penetration models are given. Base electrolyte association constants obtained with the Bjerrum theory are given. This material is available free of charge via the Internet at http://pubs.acs.org.

JA064701T